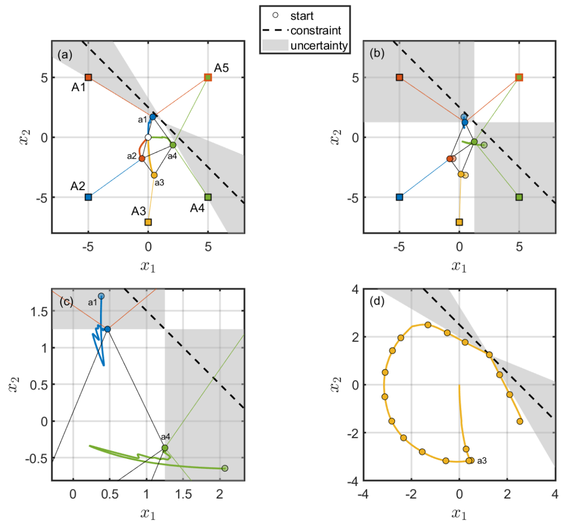

Fig. 4: Locations of agents and anchors, interactions between agents and anchors, and nominal linear constraint in Example C.

line passing through the same point. The location of the agents when the uncertainty changes is indicated by black empty circles. We note that, when the uncertainty changes, the nodes 1, 2, and 3 are located outside the new robust feasible set and, with a transient correction, move inside the robust SW quadrant for the rest of the time.

This example showcases the ability of the dynamical system to track changes online and adapt to uncertainty changes over time. We have obtained the behavior shown by appropriate scaling of the various differential equations involved. Note that the convergence is not affected by positive scaling of the differential equations. A relatively larger scaling on the dual variables in charge of the constraints makes the system response more reactive toward feasibility and more sensitive toward uncertainty changes. We leave to future research the systematic design of the optimization system for the desired real-time behavior.

VIII. Conclusions

This paper introduced a continuous-time dynamical system for solving robust optimization problems convex in the decision variable and concave in the uncertainty. The method provides solutions for problems where existing methods are intractable or computationally expensive. Future work includes applications to non-convex problems, large-scale distributed optimization and deriving convergence rates.

IX. Appendix

A. Lemma 1 [Saddle property]

Essentially, we want to show that

$$\mathcal{L}(x^\star,\lambda,u,v^\star) \le \mu \le \mathcal{L}(x,\lambda^\star,u^\star,v)\ .$$

Under Assumption 2, an optimal solution $x^\star$ exists and based on Assumption 1, this optimal solution is unique as $f_0(x,u_0)$ is strictly convex in x for any $u_0 \in \mathcal{U}_0$. Consider any optimal solution $(x^\star,\lambda^\star,u^\star,v^\star)$ for $\mathcal{RO}$ problem (17).
For each of the lower level optimizations, let

$$\eta_i = \max_{u_i\in\mathcal{U}_i} f_i(x^\star,u_i) = f_i(x^\star,u_i^\star) = \tilde{}$$

$$\mathrm{L}_i(x^\star,u_i^\star,v_i^\star),\ i\in[N]\ .$$

From the corresponding saddle property, it follows that for all $u_i,\ i\in[N]$,

$$f_i(x^\star,u_i) - (v_i^\star)^\top h_i(u_i) \le \eta_i\ . \tag{47}$$

From the upper level saddle property, for all $\lambda_i \ge 0$, $i\in[N]^+$,

$$\eta_0 + \sum_i (c_i+\lambda_i)\eta_i \le f_0(x^\star,u_0^\star) + \sum_{i=1}^N (c_i+\lambda_i^\star)\eta_i = \mu\ .$$

Substituting the lower bound on η_i, (47), in the left hand side, it follows that for all $u_i, i\in[N]$ and $\lambda_i\ge 0, i\in[N]^+$,

$$\begin{aligned}
&\mathcal{L}(x^\star,\lambda,u,v^\star)\\
=&f_0(x^\star,u_0) - (v_0^\star)^\top h_0(u_0)\\
&+\sum_{i=1}^N (c_i+\lambda_i)(f_i(x^\star,u_i) - (v_i^\star)^\top h_i(u_i))\\
\le&\ \mu\ ,
\end{aligned}$$

where we have used $c_i+\lambda_i \ge 0$. We next use lower saddle property in the other direction, namely, for all $v_i\ge 0$,

$$\begin{aligned}
\eta_i = f_i(x^\star,u_i^\star) &= f_i(x^\star,u_i^\star) - (v_i^\star)^\top h_i(u_i^\star)\\
&\le f_i(x^\star,u_i^\star) - (v_i)^\top h_i(u_i^\star)\ ,
\end{aligned}$$

which implies that for all $v_i \ge 0$, $-v_i^\top h(u^\star) \ge 0$, $i\in[N]$. Using this property and the fact that $(c_i+\lambda_i^\star)\ge 0$, it follows that for all $v_i\ge 0$, $i\in[N]^+$,

$$-(v_0)^\top h_0(u_0^\star) - \sum_{i=1}^N (c_i+\lambda_i^\star)(v_i)^\top h_i(u_i^\star) \ge 0\ . \tag{48}$$

The upper level saddle property implies

$$\mu \le f_0(x,u_0^\star) + \sum_{i=1}^N (c_i+\lambda_i^\star) f_i(x,u_i^\star)$$

for all x. Combining this with (48), we obtain

$$\begin{aligned}
\mu \le\ & f_0(x,u_0^\star) - (v_0)^\top h_0(u_0^\star)\\
&+\sum_{i=1}^N (c_i+\lambda_i^\star)(f_i(x,u_i^\star) - (v)^\top h_i(u_i^\star))\\
=&\ \mathcal{L}(x,\lambda^\star,u^\star,v)
\end{aligned}$$

for all x and $v_i\ge 0, i\in[N]$.